Acta Biochim Biophys Sin 2011, 43: 400–408 | © The Author 2011. Published by ABBS Editorial Office in association with Oxford University Press on behalf of the Institute of Biochemistry and Cell Biology, Shanghai Institutes for Biological Sciences, Chinese Academy of Sciences. DOI: 10.1093/abbs/gmr023.
Advance Access Publication 7 April 2011

Original Article

Docking-based virtual screening of potential human P2Y12 receptor antagonists

Hua Chen[1], Xianchi Dong[2,3], Minyun Zhou[2,3], Haiming Shi[1], and Xinping Luo[1*]

[1]Department of Cardiology, Huashan Hospital, Shanghai Medical College, Fudan University, Shanghai 200040, China
[2]State Key Laboratory of Molecular Biology and Research Center for Structural Biology, Institute of Biochemistry and Cell Biology, Shanghai Institutes for Biological Sciences, Chinese Academy of Sciences, Shanghai 200031, China
[3]Graduate School of Chinese Academy of Sciences, Shanghai 200031, China
*Correspondence address. Tel: +86-21-52887165; Fax: +86-21-64037268; E-mail: luoxp2007@yahoo.com.cn

Platelet plays essential roles in hemostasis and its dysregulation can lead to arterial thrombosis. P2Y12 is an important platelet membrane adenosine diphosphate receptor, and its antagonists have been widely developed as anti-coagulation agents. The current P2Y12 inhibitors available in clinical practice have not fully achieved satisfactory anti-thrombotic effects, leaving room for further improvement. To identify new chemical compounds as potential anti-coagulation inhibitors, we constructed a three-dimensional structure model of human P2Y12 by homology modeling based on the recently reported G-protein coupled receptor *Meleagris gallopavo* β1 adrenergic receptor. Virtual screening of the modeled P2Y12 against three subsets of small molecules from the ZINC database, namely lead-like, fragment-like, and drug-like, identified a number of compounds that might have high binding affinity to P2Y12. Detailed analyses of the top three compounds from each subset with the highest scores indicated that all of these compounds beard a hydrophobic bulk supplemented with a few polar atoms which bound at the ligand binding site via largely hydrophobic interactions with the receptor. This study not only provides a structure model of P2Y12 for rational design of anti-platelet inhibitors, but also identifies some potential chemicals for further development.

Keywords P2Y12; homology modeling; virtual screening; anti-coagulation

Received: November 1, 2010 Accepted: January 18, 2011

Introduction

Platelet plays essential roles in hemostasis and arterial thrombosis [1]. After thrombogenic stimuli such as vessels injury or lesions rupture in a coronary artery, platelets are activated by adhesion to the damaged sites, which further initiates a cascade of downstream signaling and ultimately leads to the occurrence of adverse cardiovascular events [2,3]. During this complicated process, a number of mediators released from the platelets and the receptors on platelet membrane are involved, among which adenosine diphosphate (ADP) and its corresponding platelet receptors are of great importance [4].

ADP, mainly secreted by erythrocytes, endothelial cells, and dense granules of stimulated platelets, serves as a powerful agonist in the platelet aggregation [5]. Effects of ADP are manifested through two distinct platelet receptors, namely P2Y1 and P2Y12 [6], both of which are purinoreceptors belonging to the G-protein coupled receptor (GPCR) family. P2Y1 is coupled to Gq [7], while P2Y12 is coupled to G_{i2} [8]. Although both P2Y1 and P2Y12 are required for the ADP-induced aggregation, they play different roles in facilitating thrombosis [9,10]. Stimulation of P2Y1 leads to intracellular calcium mobilization, platelet shape change, and transient reversible platelet aggregation [11,12]. The P2Y12-mediated ADP signaling effects include calcium mobilization, granule release, thromboxane A2 generation, and activation of glycoprotein IIb/IIIa receptor, which finally results in amplification of stable platelet aggregation and secretion [13–15]. Due to the unique role in platelet activation and aggregation, the blockage of interaction between ADP and its receptors is of great value for selective attenuation of ADP-induced platelet activation. Compared with the ubiquitously expressed P2Y1, P2Y12 is mainly found on the surface of human platelets, making it a more attractive target for the development of novel anti-platelet agents [16].

During the past years, a series of P2Y12 antagonists have been developed as drugs for the treatment of a variety of thrombotic diseases, such as stroke and myocardial infarction. Based on the chemical properties and the inhibitory mechanisms of these antagonists, they are mainly divided into two types: thienopyridines and nonthienopyridines. Thienopyridines including ticlopidine, clopidogrel, and prasugrel, have been commonly used in clinical practice nowadays [17]. In general, the thienopyridine drugs

share similar inhibitory mechanism. They all are prodrugs that have to be converted first to the active forms via hepatic cytochrome P450. The active metabolites can specifically and irreversibly bind to cysteine residues of the P2Y12 receptor and consequently inhibit the ADP-mediated platelet activation and aggregation [18]. Despite their high anti-platelet activity, certain drawbacks exist, including relatively slow-onset and considerable inter-individual variability [19]. Unlike thienopyridines, nonthienopyridines are still undergoing clinical trials. These inhibitors can directly and reversibly bind to P2Y12 independent of cytochrome P450 biotransformation, which endows them with much faster onset and more pronounced platelet inhibition [20]. Nevertheless, there are also some side effects associated with these nonthienopyridine drugs such as greater occurrence of dyspnea and ventricular pause [21]. Thus, there is need to search for new inhibitors targeting at the P2Y12 receptor.

To improve present P2Y12 antagonists and to search for new inhibitors of P2Y12, the structural information of P2Y12 is of great importance and help. However, being a transmembrane (TM) protein that is extremely difficult to crystallize, the crystal structure of P2Y12 is still unavailable. As a result, the structural basis of the interactions between the antagonists and the receptor has not been fully elucidated. With the rapid development of computational biology, homology modeling has become a powerful tool to build the structure model of a target protein [22], which can be utilized to investigate potential protein–ligand interactions and identify possible inhibitors [23]. Previously, Zhan *et al.* [24] reported a structure model of P2Y12 based on bovine rhodopsin which has barely 29% sequence similarity to human P2Y12. However, rhodopsin is not considered to be an appropriate template for P2Y12, because it is a light-sensitive receptor [25] without a typical ligand binding pocket that is important for P2Y12. Recently, the crystal structure of *Meleagris gallopavo* β1 adrenergic receptor (β1AR) was solved [26], which shares a higher sequence similarity with human P2Y12 and contains a ligand binding site. Therefore, β1AR can be used as a better template to construct a structure model of human P2Y12 for virtual screening and rational design of potential P2Y12 inhibitors.

In this study, we first constructed a 3D structure model of human P2Y12 using the turkey β1AR as the template. Virtual screening of this structure model of P2Y12 against a large library of small molecules was performed using a docking program. We identified a number of compounds that could bind to the ligand binding pocket of P2Y12. Analyses of top three compounds with the highest binding energy from three subsets of compounds, namely lead-like, fragment-like, and drug-like, revealed the properties of these compounds and their interactions with the receptor. These results can be exploited in the design and development of new inhibitors against human P2Y12.

Materials and Methods

Homology modeling of P2Y12

The amino acid sequence of human P2Y12 (NCBI accession number NP_073625.1) was used as the query sequence to search for the homolog models with known structures from the Protein Data Bank (PDB) using NCBI-BLAST [27]. *Meleagris gallopavo* β1AR has the highest sequence similarity with human P2Y12 and contains a conserved ligand binding pocket. In addition, the crystal structure of the turkey β1AR (PDB code 2VT4) was determined at 2.7 Å resolution, which provided more detailed structure information in the ligand binding pocket. Thus, the structure of the turkey β1AR assumes to be more suitable than that of rhodopsin as a template for homology modeling of human P2Y12. The 3D model of human P2Y12 was generated using program MODELLER (version 9V8) [28] that was energy minimized using the molecular dynamics simulation procedure in this program. The sequence alignment was generated using the ESPript2.2 server [29]. The quality and stereochemistry of the model were evaluated using program PROCHECK [30]. All the structure figures were generated using program Pymol [31].

Docking of known ligands and virtual screening of potential inhibitors

Chembl database is an online database containing information of the properties and activities of a large number of drugs and drug-like small molecules [32]. To validate the P2Y12 model, we docked three representative known ligands of P2Y12 from Chembl database into the putative ligand binding pocket with the program DOCK 6.0 [33]. Firstly, the modeled P2Y12 was modified by Dock Prep module implemented in program Chimera [34] to add hydrogen and charges. In this step, no clash between hydrogen atoms was observed in our model. Secondly, the small molecules were energy minimized using the Prodrg server [35], and then modified in Chimera to add hydrogen and charges. Thirdly, the molecular surface of P2Y12 was generated with program DMS [36], and the grid for the selected ligand binding pocket was calculated using DOCK 6.0. The dimension of the chosen grid was $123 \times 145 \times 103$ points which was large enough to include all residues of the putative ligand binding pocket of P2Y12. Docking was performed with flexible ligand docking parameters, while the other parameters were set to the default values.

The ZINC database was used for virtual screening, which contained a large number of commercially available compounds [37]. According to their molecular properties,

three subsets of compounds from the ZINC database were chosen for virtual screening, namely lead-like, fragment-like, and drug-like. To efficiently screen the compounds within reasonable time frames, we also chose DOCK 6.0 as the primary molecular docking program using the previously calculated grid and rigid ligand docking parameters. All of the compounds that were docked into the ligand binding pocket of P2Y12 were subjected to energy minimization, and then ranked automatically according to criteria of the interaction energy combined with geometrical matching quality. Finally, the top three compounds each from the three subsets with the highest binding energies were selected for further interaction analysis.

Results

Structure model of P2Y12

Human P2Y12 is a critical target for anti-platelet drugs. However, its crystal structure is still unavailable. To carry out virtual screening of potential inhibitors of P2Y12, we constructed a homology model of human P2Y12 based on *M. gallopavo* β1AR, which shares the highest similarity with P2Y12 among the GPCRs with known structures (sequence identity of 24% and similarity of 39% calculated using NCBI-BLAST). The structure model of P2Y12 is of high stereochemical quality with the main-chain conformations of 95.5% of the residues located in either the most favored or additionally allowed regions of the Ramachandran plot.

The structure model of P2Y12 is shown in **Fig. 1(A)**. Similar to other GPCRs, the structure model of P2Y12 was characterized by an extracellular (EL) N-terminal region, followed by seven transmembrane (TM) α-helices linked by three EL and three intracellular loops, and finally an intracellular C-terminal region. Sequence alignment and structural comparison between P2Y12 and β1AR indicated that the TM α-helices were highly conserved in both sequence and structure; however, the N-terminal region and the loop regions were less conserved [**Fig. 1(B,C)**].

Putative ligand binding pocket of P2Y12 model

Of particular interest is the ligand binding pocket of P2Y12. Site-directed mutagenesis studies have shown that the antagonists bind primarily to a similar area on the EL side of the TM segments for all GPCRs [38–40]. In addition, the EL loop EL2 of GPCRs also plays an important role in ligand binding [41]. Therefore, our docking experiments focused primarily on the TM segments and EL2 to identify the putative ligand binding pocket and the potential inhibitors.

Our docking results showed that the putative ligand binding pocket was located in the upper region of the TM segments partly covered by EL2, and was composed of residues Arg256 and Tyr259 of TM6, Phe277 and Tyr278 of TM7, and Phe182 and Leu184 of EL2. The residues forming the putative active site were highly conserved between P2Y12 and β1AR, and these residues were located either in the most favored or additionally allowed regions of the Ramachandran plot. Thus, the conformations of these residues at the active site are reliable. Also, as shown in **Fig. 1(C)**, the structural elements TM6, TM7, and EL2 that were involved in the formation of the ligand binding pocket were highly conserved between P2Y12 and β1AR, suggesting that the conformation of the ligand binding pocket of our P2Y12 model was more reliable. Moreover, our model agrees well with the available clinical and biochemical data. Specifically, our modeling studies revealed that residue Arg256 played an important role in the interaction of P2Y12 with the selected compounds (see discussion later), which was consistent with the previous studies showing that this residue was involved in the antagonist recognition. It was reported that a patient with a mutation of R256Q in P2Y12 exhibited abnormal P2Y12-dependent platelet activation [42]. Mutagenesis data also showed that Arg256 in EL2 played an important role in antagonist recognition [43].

Molecular docking and compound selection

Prior to virtual screening, the natural substrate of P2Y12 (ADP) and two known P2Y12 ligands (CHEMBL 291376 and CHEMBL 1160361) were docked into the active site to validate the putative ligand binding pocket. As shown in **Fig. 2**, the binding site of our P2Y12 model could accommodate all three ligands properly, indicating that the binding site of the P2Y12 model was suitable for further virtual screening.

Subsequently, the virtual screening of potential inhibitors against P2Y12 was carried out using program DOCK 6.0 [33] from the ZINC database [37]. Prior to docking to the putative ligand binding pocket of P2Y12, each subset of compounds was filtered by certain criteria as follows: For a total of 3 million lead-like compounds, the criteria were PlogP <3.5, molecular weight <350 Da, and number of rotatable bonds no >7. For a total of 406,730 fragment-like compounds, the criteria were PlogP <2.5, molecular weight <250 Da, and number of rotatable bonds up to 5. For a total of 13 million drug-like compounds, the criteria were PlogP <5, molecular weight from 150 to 500 Da, number of rotatable bonds up to 8, polar surface area <150 Å^2, and number of hydrogen bond acceptors up to 10.

In the docking process, P2Y12 was kept rigid, whereas the compound was sampled in, on average, 100 orientations and further energy minimized. The binding energy of the compound with the receptor was calculated as the sum of the van der Waals and electrostatic interaction

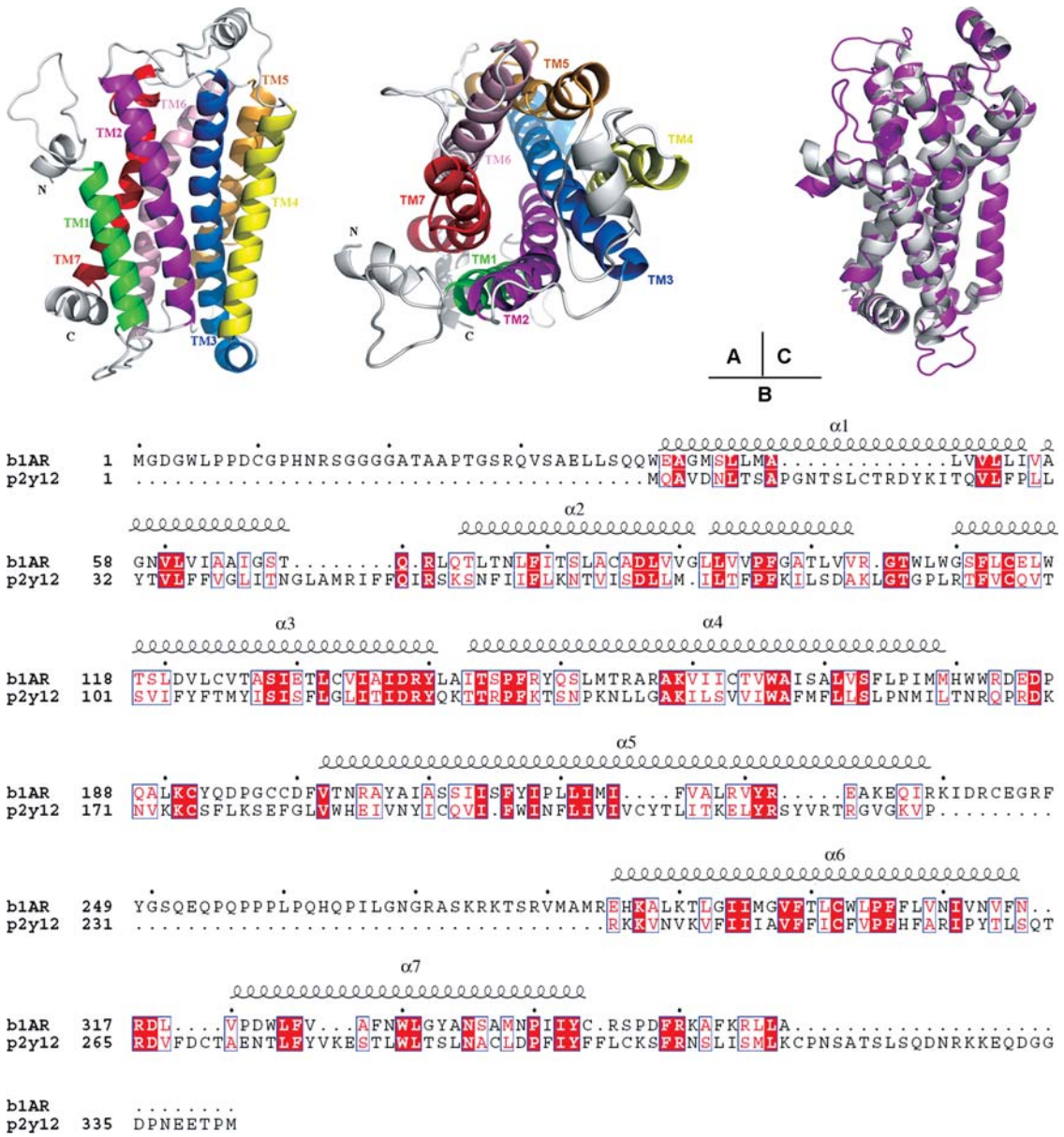

Figure 1 Representation of the structure model of human P2Y12 (A) Side and top view of the P2Y12 receptor. Seven transmembrane (TM1-7) regions are labeled in different colors. N and C represent the N- and C-terminus, respectively. (B) Sequence alignment between P2Y12 and β1AR. (C) Superposition of the structure model of P2Y12 with that of β1AR. P2Y12 is shown in magenta, while β1AR in gray.

energies. According to the energy minimization score, the top three compounds from each subset were chosen for further analysis and discussion. These nine compounds are summarized in **Table 1**. All of these compounds bear a hydrophobic bulk supplemented with a few polar atoms that bind at the putative ligand binding pocket via largely hydrophobic interactions with the receptor.

Binding of the lead-like compounds

The top three lead-like compounds identified from our virtual screening are all hydrophobic in nature, and interact with the receptor via primarily hydrophobic interactions supplemented with a few hydrophilic interactions.

For compound 1a [1-allophanoylethyl 1-(4-ethylphenyl)-5-oxo-pyrrolidine-3-carboxylate], the bulk aromatic rings formed extensive hydrophobic interactions with the aromatic side-chains of Tyr259, Phe277, and Tyr278 and the aliphatic side-chain of Leu184 [**Fig. 3(A)**]. In addition, the hydrophilic tail could form two hydrogen bonds with the side-chain of Arg256 and the main-chain carbonyl of Trp186. To increase the binding affinity of this compound with P2Y12, it might be beneficial to substitute the O1 on the middle aromatic ring with a methyl group to enhance the hydrophobic interactions. In addition, modification of the C1 with a hydrophilic group might form an extra hydrogen bond with Ser83 that may further stabilize the binding of this compound.

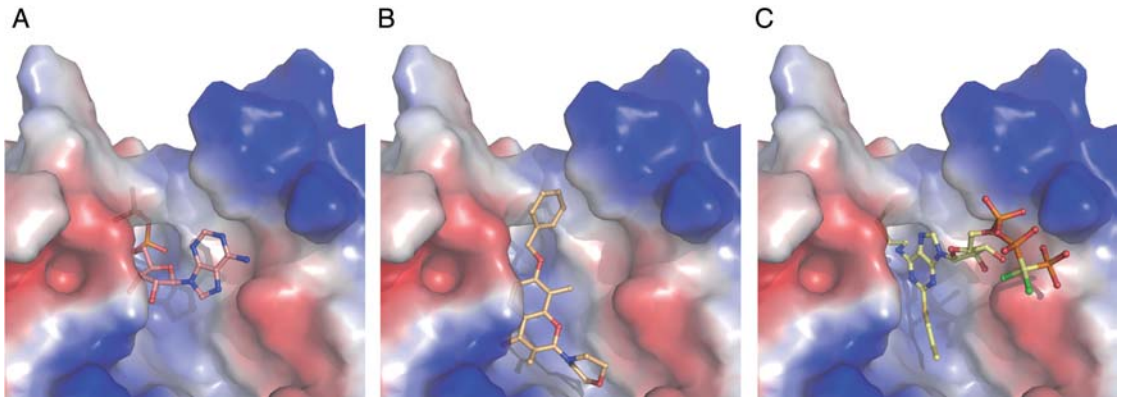

Figure 2 Docking of known ligands into the putative ligand binding pocket of P2Y12 Electrostatic surfaces of the putative ligand binding site of P2Y12 bound with (A) ADP, (B) CHEMBL291376, and (C) CHEMBL1160361. The bound ligands ADP (in limon), CHEMBL291276 (in light orange), and CHEMBL1160361 (in pale yellow) are shown in ball-and-stick models.

Table 1 Binding energy between compounds and P2Y12

Subset	Compound	ZINC code	Binding energy (kcal)			Calculated K_d (M) in 25°C
			Van der Waals	Electrostatic	Total	
Lead-like	1a	ZINC06081871	−47.38	−2.62	−50.00	1.72×10^{-9}
	1b	ZINC04782658	−46.36	−0.88	−47.24	5.24×10^{-9}
	1c	ZINC04588161	−47.46	0.23	−47.23	5.26×10^{-9}
Fragment-like	2a	ZINC03246803	−37.58	−3.65	−41.23	5.93×10^{-8}
	2b	ZINC02378695	−30.20	−9.37	−39.57	1.16×10^{-7}
	2c	ZINC04820231	−35.80	−3.63	−39.43	1.23×10^{-7}
Drug-like	3a	ZINC04993127	−51.35	−3.41	−54.76	2.52×10^{-10}
	3b	ZINC04849611	−50.33	−2.67	−53.00	5.12×10^{-10}
	3c	ZINC03841020	−52.06	0.80	−51.26	1.03×10^{-9}

Compound 1b [*N*-(7-cyclopropylcarbonylamino-9H-fluoren-2-yl) cyclopropanecarboxamide] had mainly hydrophobic interactions with P2Y12 via its phenanthrene moiety and the aromatic side-chains of Tyr259, Phe277, and Tyr278 and the aliphatic side-chain of Leu184 of the receptor [**Fig. 3(B)**]. Since residues Asn274 and Asp266 pointed their hydrophilic side-chains toward the phenanthrene moiety, modifications of the C2 and C14 on the phenanthrene ring to introduce favorable hydrophilic interactions with the receptor might stabilize the binding of compound 2b. Moreover, moderately increasing the hydrophilic property of the tail of compound 2b might also be helpful.

Compound 1c [*N*-benzyl-5-methyl-*N*-[2-(propylcarbamoyl) ethyl] pyrazine-2-carboxamide] had both hydrophobic and hydrophilic interactions with the receptor. The benzene ring interacted with the aromatic side-chains of Phe277 and Tyr278, and the aliphatic side-chain of Leu184 [**Fig. 3(C)**]. The O1 and O2 atoms formed two hydrogen bonds with the side-chain amino group of Arg256 and Asn274, respectively. Considering that this compound bound on the surface region of P2Y12, further enhancement of the hydrophilic interaction with the receptor might improve the binding affinity. Two hydrophilic residues Asp169 and Asn171 pointed their side-chains toward the pyrazine moiety with good geometry. Thus, substitution of the methyl group on the pyrazine moiety with some hydrophilic group could introduce hydrogen bonds with the receptor and thus might further stabilize the binding of compound 1c. Moreover, addition of a polar group on the C1 might also be advantageous, because it may form a hydrophilic interaction with Gln188.

Binding of the fragment-like compounds

Once again, all three fragment-like compounds comprise a hydrophobic bulk and a few polar groups. The fragment-like compounds are smaller in molecular weight and their hydrophobic interactions with P2Y12 seem not as strong as the lead-like compounds. But they have relatively more hydrophilic interactions. Also, the fragmental property of these molecules makes the modifications of them more effective and efficient.

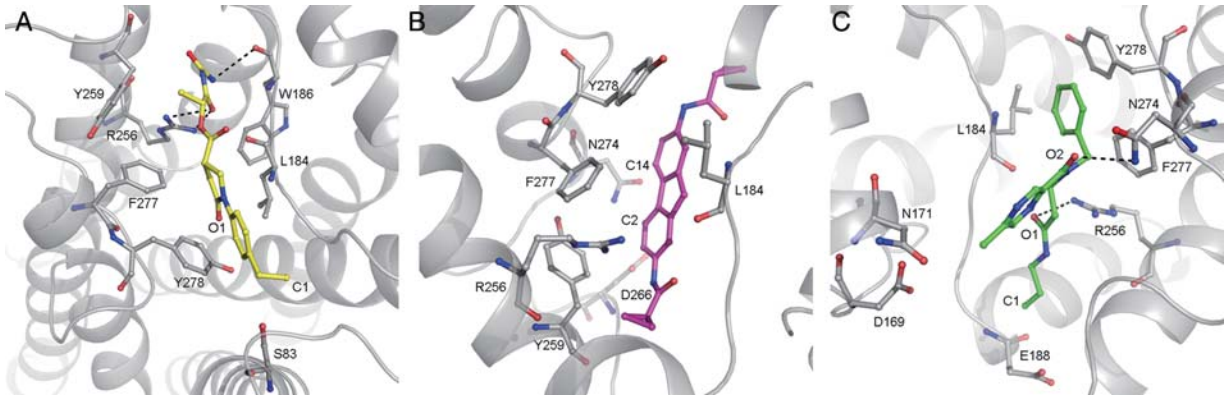

Figure 3 Structures of the binding site of the lead-like compounds (A) Interactions of compound 1a [1-allophanoylethyl 1-(4-ethylphenyl)-5-oxo-pyrrolidine-3-carboxylate] (in yellow) with P2Y12 (in gray). (B) Interactions of compound 1b [*N*-(7-cyclopropylcarbonylamino-9H-fluoren-2-yl) cyclopropanecarboxamide] (in magenta) with P2Y12 (in gray). (C) Interactions of compound 1c [*N*-benzyl-5-methyl-*N*-[2-(propylcarbamoyl) ethyl]-pyrazine-2-carboxamide] (in green) with P2Y12 (in gray). Hydrogen bonds between the compounds and P2Y12 are denoted with dashed lines.

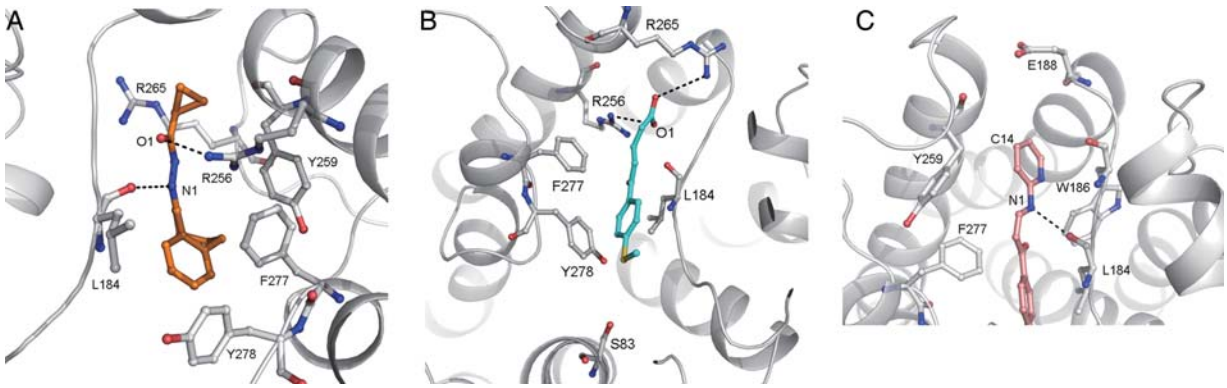

Figure 4 Structures of the binding site of the fragment-like compounds (A) Interactions of compound 2a [N′-(2-bicyclo [5.4.0] undeca-2, 8, 10, 12-tetraenyl)-cyclopropanecarbohydrazide] (in orange) with P2Y12 (in gray). (B) Interactions of compound 2b [5-(4-methylsulfanylphenyl)-5-oxo-pentanoic acid] (in cyan) with P2Y12 (in gray). (C) Interactions of compound 2c [1-(*p*-tolyl)-3-(2-pyridylamino) prop-2-en-1-one] (in pink) with P2Y12 (in gray). Hydrogen bonds and salt bridges between the compounds and P2Y12 are denoted with dashed lines.

Compound 2a [N′-(2-bicycloundeca-2, 8, 10, 12-tetraenyl) cyclopropanecarbohydrazide] had both hydrophobic and hydrophilic interactions with the receptor [**Fig. 4(A)**]. Particularly, the head of the compound made extensive hydrophobic contacts with Phe277, Tyr278, and Leu184. The O1 atom formed a hydrogen bond with the side-chain of Arg256, and the N1 atom formed a hydrogen bond with the main-chain carbonyl of Leu184. As the cyclopropane moiety of compound 2a was oriented toward a hydrophilic region, addition of some polar atoms to this group might enhance favorable ligand–receptor interactions.

Compound 2b [5-(4-methylsulfanylphenyl)-5-oxo-pentanoic acid] is relatively smaller. Its aromatic ring made hydrophobic interactions with the aromatic side-chain of Phe277 and the aliphatic side-chain of Leu184, and its carboxyl group formed two salt bridges with the side-chain amides of Arg256 and Arg265 [**Fig. 4(B)**]. Since the O1 group pointed toward a hydrophobic pocket, alteration of the O1 to certain hydrophobic groups might improve the binding affinity of this compound. Moreover, appropriate modification of the S1 group might also be advantageous in enhancing the interaction between the ligand and the receptor by forming a hydrogen bond with the side-chain hydroxyl of Ser83.

For compound 2c [1-(*p*-tolyl)-3-(2-pyridylamino)prop-2-en-1-one], its benzene ring was sandwiched between the aromatic side-chains of Trp186, Phe277, and Tyr278, and its pyridine moiety had hydrophobic interactions with the aromatic side-chains of Trp186 and Tyr259 as well [**Fig. 4(C)**]. In addition, the N1 atom formed a hydrogen bond with the main-chain carbonyl of Leu184. Considering the empty space between the pyridine moiety of the compound and the flexible side-chain of Glu188, addition of certain hydrophilic substituent at the C14 position of the compound might introduce a salt bridge or hydrogen bond and thus increased the binding affinity and specificity.

Binding of the drug-like compounds

The drug-like compounds comprise several functional moieties with relatively larger molecular weights, and thus their interactions with the receptor are stronger.

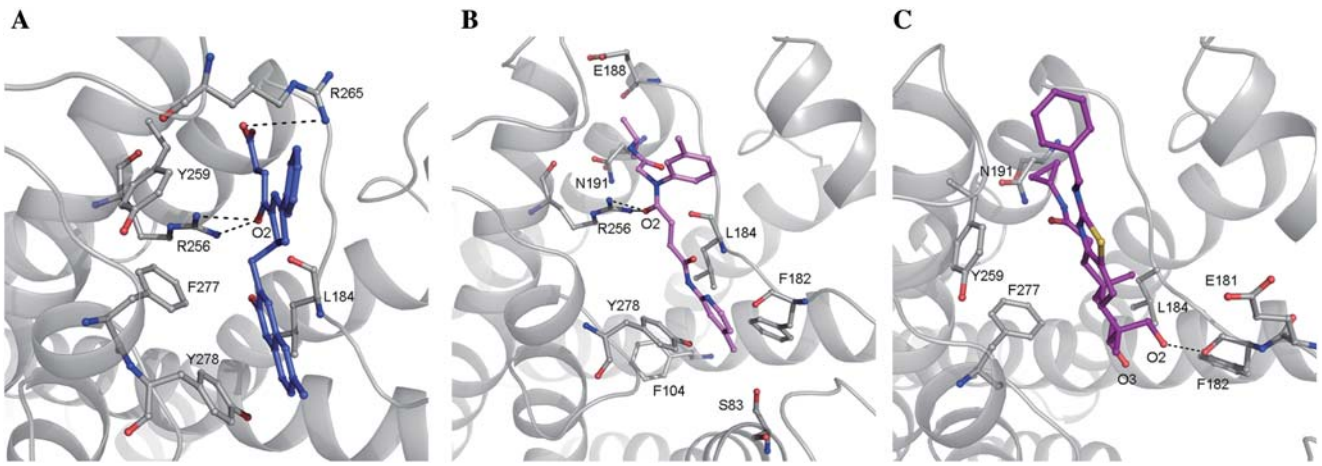

Figure 5 Structures of the binding site of the drug-like compounds (A) Interactions of compound 3a [4-[5-[(6-methyl-2-oxo-1H-quinolin-3-yl) methyl]-3-phenyl-4,5-dihydropyrazol-1-yl]-4-oxo-butanoic acid] (in blue) with P2Y12 (in gray). (B) Interactions of compound 3b [*N*-(isopropylcarbamoylmethyl)-*N*′-(4-methyl-2-pyridyl)-*N*-(*m*-tolyl)butanediamide] (in violet) with P2Y12 (in gray). (C) Interactions of compound 3c [2-[benzylamino-hydroxy-(hydroxymethyl)-dimethyl-BLAHyl]-*N*-cyclopropyl-acetamide] (in magenta) with P2Y12 (in gray). Hydrogen bonds and salt bridges between the compounds and P2Y12 are denoted with dashed lines.

For compound 3a [4-[5-[(6-methyl-2-oxo-1H-quinolin-3-yl) methyl]-3-phenyl-4, 5-dihydropyrazol-1-yl]-4-oxo-butanoic acid], the naphthol moiety made extensive hydrophobic interactions with the aromatic side-chains of Phe277 and Tyr278 and the aliphatic side-chain of Leu184, and the cyclopentane moiety made hydrophobic interactions with the aromatic side-chain of Tyr259 [**Fig. 5(A)**]. The O2 atom formed two hydrogen bonds with the side-chain of Arg256, and the carbonyl group formed a salt bridge with the side-chain of Arg265. Since the benzene ring of compound 3a pointed toward the hydrophilic region on the outer surface of P2Y12, substitution of this hydrophobic group with certain hydrophilic group might further stabilize the binding of the ligand with the receptor.

For compound 3b [*N*-(isopropylcarbamoylmethyl)-*N*′-(4-methyl-2-pyridyl)-*N*-(*m*-tolyl)butanediamide], the pyridine moiety was sandwiched between the aromatic side-chains of Phe104, Phe182, and Tyr278 and the aliphatic side-chain of Leu184 [**Fig. 5(B)**]. The O2 atom made hydrophilic interaction with the side-chain amino group of Arg256. Considering that the pyricline ring pointed toward a hydrophilic region, modification of this ring with some polar groups might introduce a hydrogen-bonding interaction with the side-chain of Ser83, and consequently enhanced its interaction with the receptor. In addition, replacement of the methylene group by some hydrophilic ones might also introduce some salt bridges or hydrogen bonds between the ligand and the side-chain of Asp191 and/or Glu188.

Compound 3c [2-[benzylamino-hydroxy-(hydroxymethyl)-dimethyl-BLAHyl]-*N*-cyclopropyl-acetamide] had relatively weaker interactions with P2Y12. Its hydrophobic moieties made some hydrophobic contacts with the aromatic side-chains of Tyr259 and Phe277 and the aliphatic side-chain of Leu184, and its O2 atom formed a hydrogen bond with the main-chain carbonyl of Phe182 [**Fig. 5(C)**]. To increase its binding affinity, some modifications can be considered. For example, improving the hydrophobic character of the O3 position can strengthen its interactions with the receptor. Also, modification of the cyclopropane moiety with some hydrophilic groups may add hydrophilic interactions with Asn191. Since the benzene ring points toward the outer hydrophilic region of P2Y12, substitution of this moiety with some hydrophilic groups may be helpful in stabilizing the interactions between compound 3c and P2Y12.

In summary, based on our modeled structure of P2Y12, our virtual screening against a large library of small molecules identified several compounds that may have high binding affinity with the receptor. Structural analysis of the top three compounds with the highest binding energy in the three subsets of compounds, namely lead-like, fragment-like, and drug-like, revealed that all these compounds were composed of a bulk hydrophobic core with several hydrophilic groups and could interact with P2Y12 mainly via hydrophobic interactions supplemented with certain hydrophilic interactions. This work provides the structural basis for further rational design of novel anti-platelet inhibitors.

Discussion

GPCRs are a large family of TM proteins that are of great biological importance, and thus are targets for therapeutic drug design [44]. However, due to the difficulty in obtaining 3D structures, computational methods, such as homology modeling, can provide an alternative way in the structural and functional studies of GPCRs and their interactions with ligands, because these membrane proteins are structurally more conserved than sequences. P2Y12 is an

essential target of anti-platelet agents; however, its 3D structure is unavailable and the structure basis for its antagonist binding is unclear. In this study we carried out the modeling study of P2Y12 and the docking-based virtual screening of potential antagonists against P2Y12.

Homology modeling is based on the reasonable assumption that two homologous proteins will share very similar structures [45]. Because the sequence identity between P2Y12 and those GPCRs with known 3D structures is relatively low, modeling of P2Y12 is highly challenging [46]. Here, the homology model of human P2Y12 was constructed using *M. gallopavo* β1AR as the template, which shared the highest similarity with P2Y12 among the GPCRs with available structures (sequence identity of 24%), and thus was assumed to be better than the previously reported model of P2Y12 [24]. Considering that the homology model cannot be as accurate as the crystal structure, before virtual screening, we firstly validated whether our model of P2Y12 especially the ligand binding pocket was reliable. Three known ligands were docked into the putative ligand binding pocket of P2Y12, and the results showed that the binding pocket could accommodate all three ligands properly, indicating that our P2Y12 model was accurate and suitable for further virtual screening.

Virtual screening, which uses computational algorithms and models for the identification of novel bioactive molecules, is emerging as an important tool in modern drug discovery [47]. Comparing with traditional high-throughput biochemical compound screening, virtual screening bears some merits. First, virtual screening saves money and time. The experimental costs for the synthesis and biological screening of millions or billions of compounds are still considerably high. While virtual screening is much cheaper and is able to process much more compounds in less time, by restricting itself to libraries of specific, accessible compounds [48]. Second, virtual screening can provide visual analysis of the receptor–ligand interactions, which allows for an intuitive interpretation of the binding process at the binding site of the receptor. Based on the screening information, modifications of compounds can also be easily performed to strengthen their binding affinities [49]. Recently, virtual screening has been widely used in the GPCR field with several successful applications of GPCR models in virtual screening [50–52], indicating the general relevance of GPCR models and their usefulness for structure-based drug design [53]. In this study, we identified a number of compounds that might have high binding affinity to P2Y12. The detailed analyses of the P2Y12–compound interactions showed that all compounds were composed of a bulk hydrophobic core with several hydrophilic groups, and interacted with P2Y12 via mainly hydrophobic interactions supplemented with certain hydrophilic interactions. Furthermore, several key residues, which were identified by previous clinical and biochemical studies, were observed to play important roles in the P2Y12–compound interactions, further affirming the reliability of our virtual screening. Based on the detailed interaction information, modifications that might enhance the P2Y12–compound interaction for each selected compound were proposed, which can provide useful structural clues for further rational drug design. It is noteworthy to point out that since the binding affinity of P2Y12 with each selected compound is not measured experimentally, considering that virtual screening may yield false-positive results, further experiments are needed in the future to evaluate these P2Y12–compound interactions.

Acknowledgements

We thank other members of our groups for helpful suggestion and discussion. We are also grateful to Professor Jianping Ding for his support to this work and his critical reading of the manuscript.

Funding

This work was supported by a grant from the National Natural Science Foundation of China (30972965).

References

1 Ruggeri ZM. Platelets in atherothrombosis. Nat Med 2002, 8: 1227–1234.
2 Jackson SP, Nesbitt WS and Kulkarni S. Signaling events underlying thrombus formation. J Thromb Haemost 2003, 1: 1602–1612.
3 Davies MJ and Thomas A. Thrombosis and acute coronary-artery lesions in sudden cardiac ischemic death. N Engl J Med 1984, 310: 1137–1140.
4 Born GV. Aggregation of blood platelets by adenosine diphosphate and its reversal. Nature 1962, 194: 927–929.
5 Cattaneo M, Lombardi R, Zighetti ML, Gachet C, Ohlmann P, Cazenave JP and Mannucci PM. Deficiency of (33P)2MeS-ADP binding sites on platelets with secretion defect, normal granule stores and normal thromboxane A2 production. Evidence that ADP potentiates platelet secretion independently of the formation of large platelet aggregates and thromboxane A2 production. J Thromb Haemost 1997, 77: 986–990.
6 Mills DC. ADP receptors on platelets. J Thromb Haemost 1996, 76: 835–856.
7 Savi P, Beauverger P, Labouret C, Delfaud M, Salel V, Kaghad M and Herbert JM. Role of P2Y1 purinoceptor in ADP-induced platelet activation. FEBS Lett 1998, 422: 291–295.
8 Ohlmann P, Laugwitz KL, Nurnberg B, Spicher K, Schultz G, Cazenave JP and Gachet C. The human platelet ADP receptor activates Gi2 proteins. Biochem J 1995, 312: 775–779.
9 Jantzen HM, Gousset L, Bhaskar V, Vincent D, Tai A, Reynolds EE and Conley PB. Evidence for two distinct G-protein-coupled ADP receptors mediating platelet activation. J Thromb Haemost 1999, 81: 111–117.
10 Jin J and Kunapuli SP. Coactivation of two different G protein-coupled receptors is essential for ADP-induced platelet aggregation. Proc Natl Acad Sci USA 1998, 95: 8070–8074.
11 Daniel JL, Dangelmaier C, Jin J, Ashby B, Smith JB and Kunapuli SP. Molecular basis for ADP-induced platelet activation. I. Evidence for three

distinct ADP receptors on human platelets. J Biol Chem 1998, 273: 2024–2029.
12 Jin J, Daniel JL and Kunapuli SP. Molecular basis for ADP-induced platelet activation. II. The P2Y1 receptor mediates ADP-induced intracellular calcium mobilization and shape change in platelets. J Biol Chem 1998, 273: 2030–2034.
13 Daniel JL, Dangelmaier C, Jin J, Kim YB and Kunapuli SP. Role of intracellular signaling events in ADP-induced platelet aggregation. J Thromb Haemost 1999, 82: 1322–1326.
14 Paul BZ, Jin J and Kunapuli SP. Molecular mechanism of thromboxane A(2)-induced platelet aggregation. Essential role for p2t(ac) and alpha(2a) receptors. J Biol Chem 1999, 274: 29108–29114.
15 Michelson AD. P2Y12 antagonism: promises and challenges. Arterioscler Thromb Vasc Biol 2008, 28: s33–s38.
16 Hollopeter G, Jantzen HM, Vincent D, Li G, England L, Ramakrishnan V and Yang RB, *et al*. Identification of the platelet ADP receptor targeted by antithrombotic drugs. Nature 2001, 409: 202–207.
17 Porto I, Giubilato S, De Maria GL, Biasucci LM and Crea F. Platelet P2Y12 receptor inhibition by thienopyridines: status and future. Expert Opin Investig Drugs 2009, 18: 1317–1332.
18 Farid NA, Kurihara A and Wrighton SA. Metabolism and disposition of the thienopyridine antiplatelet drugs ticlopidine, clopidogrel, and prasugrel in humans. J Clin Pharmacol 2010, 50: 126–142.
19 Husted S. Unmet needs in oral antiplatelet therapy with ADP receptor blocking agents. Fundam Clin Pharmacol 2009, 23: 1–9.
20 Angiolillo DJ and Guzman LA. Clinical overview of promising nonthienopyridine antiplatelet agents. Am Heart J 2008, 156: 23–28.
21 Michelson AD. Antiplatelet therapies for the treatment of cardiovascular disease. Nat Rev Drug Discov 2010, 9: 154–169.
22 Hillisch A, Pineda LF and Hilgenfeld R. Utility of homology models in the drug discovery process. Drug Discov Today 2004, 9: 659–669.
23 Kitchen DB, Decornez H, Furr JR and Bajorath J. Docking and scoring in virtual screening for drug discovery: methods and applications. Nat Rev Drug Discov 2004, 3: 935–949.
24 Zhan C, Yang J, Dong XC and Wang YL. Molecular modeling of purinergic receptor P2Y12 and interaction with its antagonists. J Mol Graph 2007, 26: 20–31.
25 Palczewski K, Kumasaka T, Hori T, Behnke CA, Motoshima H, Fox BA and Le Trong I, *et al*. Crystal structure of rhodopsin: a G-protein-coupled receptor. Science 2000, 289: 739–745.
26 Warne T, Serrano-Vega MJ, Baker JG, Moukhametzianov R, Edwards PC, Henderson R and Leslie AG, *et al*. Structure of a beta1-adrenergic G-protein-coupled receptor. Nature 2008, 454: 486–491.
27 Altschul SF, Gish W, Miller W, Myers EW and Lipman DJ. Basic local alignment search tool. J Mol Biol 1990, 215: 403–410.
28 Eswar N, Webb B, Marti-Renom MA, Madhusudhan MS, Eramian D, Shen MY and Pieper U, *et al*. Comparative protein structure modeling using MODELLER. Curr Protoc Protein Sci 2007, S50: 2.9.1–2.9.31.
29 Gouet P, Courcelle E, Stuart DI and Metoz F. ESPript: analysis of multiple sequence alignments in PostScript. Bioinformatics 1999, 15: 305–308.
30 Laskowski RA, MacArthur MW, Moss DS and Thornton JM. PROCHECK: a program to check the stereochemical quality of protein structures. J Appl Crystallogr 1993, 26: 283–291.
31 DeLano WL and Lam JW. PyMOL: a communications tool for computational models. Abstr Pap Am Chem Soc 2005, 230: 1371–1372.
32 Bender A. DATABASES Compound bioactivities go public. Nat Chem Biol 2010, 6: 309.
33 Kuntz ID, Blaney JM, Oatley SJ, Langridge R and Ferrin TE. A geometric approach to macromolecule–ligand interactions. J Mol Biol 1982, 161: 269–288.
34 Pettersen EF, Goddard TD, Huang CC, Couch GS, Greenblatt DM, Meng EC and Ferrin TE. UCSF chimera—a visualization system for exploratory research and analysis. J Comput Chem 2004, 25: 1605–1612.
35 Schuttelkopf AW and van Aalten DMF. PRODRG: a tool for high-throughput crystallography of protein–ligand complexes. Acta Crystallogr D Biol Crystallogr 2004, 60: 1355–1363.
36 Richards FM. Areas, volumes, packing, and protein-structure. Annu Rev Biophys Bioeng 1977, 6: 151–176.
37 Irwin JJ and Shoichet BK. ZINC—a free database of commercially available compounds for virtual screening. J Chem Inf Model 2005, 45: 177–182.
38 Becker OM, Marantz Y, Shacham S, Inbal B, Heifetz A, Kalid O and Bar-Haim S, *et al*. G protein-coupled receptors: in silico drug discovery in 3D. Proc Natl Acad Sci USA 2004, 101: 11304–11309.
39 Kratochwil NA, Malherbe P, Lindemann L, Ebeling M, Hoener MC, Muhlemann A and Porter RH, *et al*.. An automated system for the analysis of G protein-coupled receptor transmembrane binding pockets: alignment, receptor-based pharmacophores, and their application. J Chem Inf Model 2005, 45: 1324–1336.
40 Jacob L, Hoffmann B, Stoven V and Vert JP. Virtual screening of GPCRs: an in silico chemogenomics approach. BMC Bioinformatics 2008, 9: 363.
41 Avlani VA, Gregory KJ, Morton CJ, Parker MW, Sexton PM and Christopoulos A. Critical role for the second extracellular loop in the binding of both orthosteric and allosteric G protein-coupled receptor ligands. J Biol Chem 2007, 282: 25677–25686.
42 Cattaneo M, Zighetti ML, Lombardi R, Martinez C, Lecchi A, Conley PB and Ware J, *et al*. Molecular bases of defective signal transduction in the platelet P2Y(12) receptor of a patient with congenital bleeding. Proc Natl Acad Sci USA 2003, 100: 1978–1983.
43 Mao Y, Zhang L, Jin J, Ashby B and Kunapuli SP. Mutational analysis of residues important for ligand interaction with the human P2Y(12) receptor. Eur J Pharmacol 2010, 644: 10–16.
44 Flower DR. Modelling G-protein-coupled receptors for drug design. Biochim Biophys Acta 1999, 1422: 207–234.
45 Patny A, Desai PV and Avery MA. Homology modeling of G-protein-coupled receptors and implications in drug design. Curr Med Chem 2006, 13: 1667–1691.
46 Reddy Ch S, Vijayasarathy K, Srinivas E, Sastry GM and Sastry GN. Homology modeling of membrane proteins: a critical assessment. Comput Biol Chem 2006, 30: 120–126.
47 Schneider G. Virtual screening: an endless staircase? Nat Rev Drug Discov 2010, 9: 273–276.
48 Shoichet BK. Virtual screening of chemical libraries. Nature 2004, 432: 862–865.
49 Klebe G. Virtual ligand screening: strategies, perspectives and limitations. Drug Discov Today 2006, 11: 580–594.
50 Bissantz C, Bernard P, Hibert M and Rognan D. Protein-based virtual screening of chemical databases. II. Are homology models of G-protein coupled receptors suitable targets? Proteins 2003, 50: 5–25.
51 Evers A and Klabunde T. Structure-based drug discovery using GPCR homology modeling: successful virtual screening for antagonists of the alpha1A adrenergic receptor. J Med Chem 2005, 48: 1088–1097.
52 Evers A and Klebe G. Successful virtual screening for a submicromolar antagonist of the neurokinin-1 receptor based on a ligand-supported homology model. J Med Chem 2004, 47: 5381–5392.
53 Evers A, Hessler G, Matter H and Klabunde T. Virtual screening of biogenic amine-binding G-protein coupled receptors: comparative evaluation of protein- and ligand-based virtual screening protocols. J Med Chem 2005, 48: 5448–5465.